On a Screw Dislocation Interacting With Two Viscous Interfaces

X. Wang[1]
e-mail: xuwang_sun@hotmail.com

E. Pan
e-mail: pan2@uakron.edu

Department of Civil Engineering,
and Department of Applied Mathematics,
University of Akron,
Akron, OH 44325-3905

We investigate a screw dislocation interacting with two concentric circular linear viscous interfaces. The inner viscous interface is formed by the circular inhomogeneity and the interphase layer, and the outer viscous interface by the interphase layer and the unbounded matrix. The time-dependent stresses in the inhomogeneity, interphase layer, and unbounded matrix induced by the screw dislocation located within the interphase layer are derived. Also obtained is the time-dependent image force on the screw dislocation due to its interaction with the two viscous interfaces. It is found that when the interphase layer is more compliant than both the inhomogeneity and the matrix, three transient equilibrium positions (two are unstable and one is stable) for the dislocation can coexist at a certain early time moment. If the inhomogeneity and matrix possess the same shear modulus, and the characteristic times for the two viscous interfaces are also the same, a fixed equilibrium position always exists for the dislocation. In addition, when the interphase layer is stiffer than the inhomogeneity and matrix, the fixed equilibrium position is always an unstable one; on the other hand, when the interface layer is more compliant than the inhomogeneity and matrix, the nature of the fixed equilibrium position depends on the time: the fixed equilibrium position is a stable one if the time is below a critical value, and it is an unstable one if the time is above the critical value. In addition, a saddle point transient equilibrium position for the dislocation can also be observed under certain conditions. [DOI: 10.1115/1.3112743]

Keywords: three-phase fibrous composite, viscous interface, screw dislocation, image force, transient equilibrium position

1 Introduction

It is well known that the interphase layer between the fiber and the surrounding matrix exerts a significant influence on the local and overall mechanical behaviors of fibrous composites [1–3]. In earlier modeling attempts [1–3], the interphase layer was assumed to be perfectly bonded to the fiber and the surrounding matrix, i.e., all the tractions and the displacements are continuous across the interfaces between two different bonded phases. However, at the microscopic level, the interface between two different bonded phases is generally not a perfect one but is with waviness or steps. At elevated temperatures, diffusional transport becomes important on these rough interfaces due to the differences in the normal tractions that are present along the rough interfaces [4,5]. It was suggested [4–8] that the microscopically mass diffusion-controlled mechanism can be macroscopically described by the linear law for a viscous interface: $\dot{\delta}=\tau/\eta$, where $\dot{\delta}$ is the sliding velocity (i.e., the differentiation of the relative sliding with respect to time t), τ is the interfacial shear stress, and η is the interfacial viscosity. Recently, the influence of the interfacial viscosity on the mechanical behaviors of composite has been addressed (see, for example, Refs. [9–12]). In addition, it was recently verified that the heterostructures in which composition/doping are modulated at the *nanometer scale* can be realized in core-shell nanowires [13]. If these core-shell nanowires are then reinforced in a metal matrix, then the three-phase cylindrical model, which will be studied in this research, becomes more relevant.

The objective of this research is to incorporate the Newtonian viscosity into the inner interface between the fiber and interphase layer and the outer interface between the interphase layer and the matrix. More specifically, we investigate in this work a screw dislocation in an annular interphase layer of uniform thickness bonded through Newtonian viscous interfaces to a circular inhomogeneity and to the surrounding unbounded matrix. It was recently observed that it is possible to find a transient equilibrium position for a screw dislocation interacting with a circular viscous interface [11]. Then it is expected that some more complex and more interesting phenomena may exist when a screw dislocation interacts with not one but two nearby viscous interfaces. Due to the fact that we consider two viscous interfaces, then it is only possible to arrive at series form solutions for this interaction problem. This paper is structured as follows. In Sec. 2, we derive the time-dependent stress field induced by the screw dislocation by means of the complex variable method. It is observed that the unknowns are determined by solving a decoupled set of state-space equations. In Sec. 3, we first obtain an expression for the time-dependent image force on the dislocation due to its interaction with the two nearby viscous interfaces; then we calculate and discuss in detail the time-dependent image force, with the focus on finding the possible transient equilibrium positions for the dislocation on which the image force is zero at a certain moment.

2 Formulation

In this section, we will analyze the time-dependent stress field associated with a three-phase circular inhomogeneity with two concentric circular linear viscous interfaces, as shown in Fig. 1. The linearly elastic materials occupying the inhomogeneity, the interphase layer, and the matrix are assumed to be homogeneous and isotropic with the associated shear moduli μ_1, μ_2, and μ_3, respectively. We represent the matrix by the domain $S_3: x^2+y^2 \geq b^2$ and assume that the circular inhomogeneity occupies the

[1]Corresponding author.

Contributed by the Applied Mechanics Division of ASME for publication in the JOURNAL OF APPLIED MECHANISM. Manuscript received May 2, 2008; final manuscript received October 3, 2008; published online June 17, 2009. Review conducted by Anthony Wass.

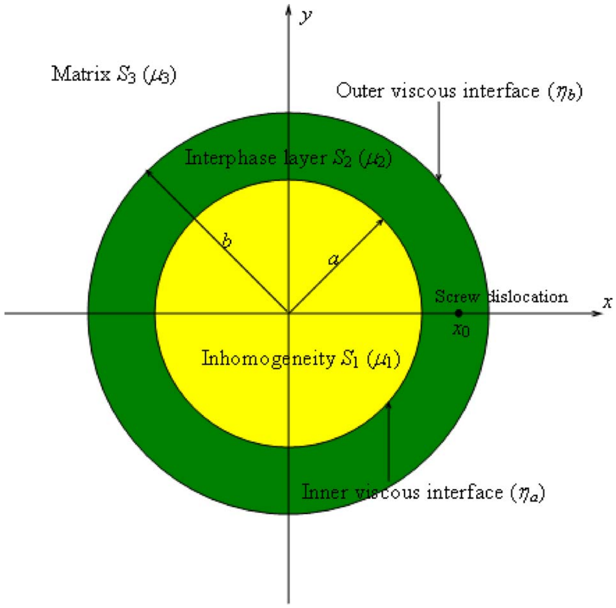

Fig. 1 A screw dislocation in a three-phase circular inhomogeneity with two concentric circular linear viscous interfaces

circular region $S_1: x^2+y^2 \leq a^2$, and the interphase layer occupies the annulus $S_2: a^2 \leq x^2+y^2 \leq b^2$. Furthermore at time $t=0$, a screw dislocation with Burgers vector b_z is introduced into the interphase layer S_2 and fixed at $[x_0, 0]$, $(a < x_0 < b)$ on the positive real axis. Throughout this paper, the subscripts 1, 2, and 3 (or the superscripts (1), (2), and (3)) are used to identify the quantities in S_1, S_2, and S_3, respectively. In this research, the inertia force in the inhomogeneity, the interphase layer, and the matrix is ignored in order to simplify the analysis involved. As such, the out-of-plane displacement w, the stress components σ_{zx} and σ_{zy} in the Cartesian coordinate system, and the stress components σ_{zr} and $\sigma_{z\theta}$ in the polar coordinate system can be expressed in terms of a single analytic function $f(z,t)$ as [14]

$$w = \mathrm{Im}\{f(z,t)\}$$

$$\sigma_{zy} + i\sigma_{zx} = \mu f'(z,t)$$

$$\sigma_{z\theta} + i\sigma_{zr} = \mu e^{i\theta} f'(z,t) \tag{1}$$

where μ is the shear modulus, t is the real time variable while $z = x+iy = re^{i\theta}$ is the complex variable, and $f'(z,t) = \partial f(z,t)/\partial z$. The appearance of the real time variable t in the analytic function f is due to the influence of the two viscous interfaces at $r=a$ and $r=b$.

The boundary conditions on the two linear viscous interfaces $r=a$ and $r=b$ can be described by

$$\sigma_{zr}^{(1)} = \sigma_{zr}^{(2)} = \eta_a(\dot{w}^{(2)} - \dot{w}^{(1)}), \quad r=a, \quad t>0$$

$$\sigma_{zr}^{(3)} = \sigma_{zr}^{(2)} = \eta_b(\dot{w}^{(3)} - \dot{w}^{(2)}), \quad r=b, \quad t>0 \tag{2}$$

where an overdot denotes the derivative with respect to the time t, and η_a and η_b are the non-negative viscosity coefficients for the two interfaces, respectively.

In view of Eq. (1), the above set of boundary conditions on the two viscous interfaces can also be expressed in terms of three analytic functions—$f_1(z,t)$ defined in the circular inhomogeneity, $f_2(z,t)$ defined in the interphase layer, and $f_3(z,t)$ defined in the unbounded matrix as

$$\mu_1 f_1^+(z,t) + \mu_1 \bar{f}_1^-\left(\frac{a^2}{z},t\right) = \mu_2 f_2^-(z,t) + \mu_2 \bar{f}_2^+\left(\frac{a^2}{z},t\right) \tag{3a}$$

$$\dot{f}_2^-(z,t) - \dot{\bar{f}}_2^+\left(\frac{a^2}{z},t\right) - \dot{f}_1^+(z,t) + \dot{\bar{f}}_1^-\left(\frac{a^2}{z},t\right)$$
$$= \frac{\mu_1}{a\eta_a}\left[z f_1'^+(z,t) - \frac{a^2}{z}\bar{f}_1'^-\left(\frac{a^2}{z},t\right)\right], \quad |z|=a \tag{3b}$$

and

$$\mu_2 f_2^+(z,t) + \mu_2 \bar{f}_2^-\left(\frac{b^2}{z},t\right) = \mu_3 f_3^-(z,t) + \mu_3 \bar{f}_3^+\left(\frac{b^2}{z},t\right) \tag{4a}$$

$$\dot{f}_3^-(z,t) - \dot{\bar{f}}_3^+\left(\frac{b^2}{z},t\right) - \dot{f}_2^+(z,t) + \dot{\bar{f}}_2^-\left(\frac{b^2}{z},t\right)$$
$$= \frac{\mu_3}{b\eta_b}\left[z f_3'^-(z,t) - \frac{b^2}{z}\bar{f}_3'^+\left(\frac{b^2}{z},t\right)\right], \quad |z|=b \tag{4b}$$

where the superscript "+" denotes approaching the interface from inside, while the superscript "−" denotes approaching the interface from outside.

We first consider the inner viscous interface. It follows from Eq. (3a) for the continuity condition of traction across the inner viscous interface $|z|=a$ that

$$f_2(z,t) = \frac{\mu_1}{\mu_2}\bar{f}_1\left(\frac{a^2}{z},t\right) + \frac{1}{\mu_2}\sum_{n=1}^{+\infty}[A_n(t)z^n - a^{2n}A_n(t)z^{-n}]$$
$$+ \frac{b_z}{2\pi}\ln(z-x_0) - \frac{b_z}{2\pi}\ln\left(\frac{z-a^2/x_0}{z}\right), \quad a<|z|<b$$

$$\bar{f}_2\left(\frac{a^2}{z},t\right) = \frac{\mu_1}{\mu_2}f_1(z,t) - \frac{1}{\mu_2}\sum_{n=1}^{+\infty}[A_n(t)z^n - a^{2n}A_n(t)z^{-n}]$$
$$- \frac{b_z}{2\pi}\ln(z-x_0) + \frac{b_z}{2\pi}\ln\left(\frac{z-a^2/x_0}{z}\right), \quad \frac{a^2}{b}<|z|<a \tag{5}$$

where $A_n(t)$ $(n=1,2,\ldots,+\infty)$ are real but time-dependent coefficients to be determined.

Substituting Eq. (5) into Eq. (3b), we obtain the following:

$$\frac{\mu_1}{a\eta_1}z f_1'^+(z,t) + \frac{\mu_1+\mu_2}{\mu_2}\dot{f}_1^+(z,t) - \frac{2}{\mu_2}\sum_{n=1}^{+\infty}\dot{A}_n(t)z^n = \frac{\mu_1}{a\eta_1}\frac{a^2}{z}\bar{f}_1'^-\left(\frac{a^2}{z},t\right)$$
$$+ \frac{\mu_1+\mu_2}{\mu_2}\dot{\bar{f}}_1^-\left(\frac{a^2}{z},t\right) - \frac{2}{\mu_2}\sum_{n=1}^{+\infty}a^{2n}\dot{A}_n(t)z^{-n}, \quad |z|=a \tag{6}$$

Apparently the left-hand side of Eq. (6) is analytic and single valued within the circle $|z|=a$, while the right-hand side of Eq. (6) is analytic and single-valued outside the circle including the point at infinity. By employing Liouville's theorem, the left- and right-hand sides should be identically zero. Consequently, we arrive at the following inhomogeneous first-order partial differential equation for $f_1(z,t)$:

$$z f_1'(z,t) + t_1\dot{f}_1(z,t) = \frac{2a\eta_a}{\mu_1\mu_2}\sum_{n=1}^{+\infty}\dot{A}_n(t)z^n, \quad |z|<a \tag{7}$$

where $t_1 = a\eta_a(\mu_1+\mu_2)/\mu_1\mu_2 > 0$ is the characteristic time for the inner viscous interface $|z|=a$.

Equation (7) can be easily solved by using power series expansion as

$$f_1(z,t) = \frac{1}{\mu_1}\sum_{n=1}^{+\infty}B_n(t)z^n, \quad |z|<a \tag{8}$$

where $B_n(t)$ is related to $A_n(t)$ through the following:

$$nB_n(t)+t_1\dot{B}_n(t)=t_1\Gamma_1\dot{A}_n(t)\quad (n=1,2,\ldots,+\infty) \tag{9}$$

with $\Gamma_1=2\mu_1/(\mu_1+\mu_2)$ $(0\le\Gamma_1\le 2)$ being a measure of the relative stiffness of the inhomogeneity with respect to the interphase layer.

Once we obtain $f_1(z,t)$, it is not difficult to arrive at the expression of $f_2(z,t)$ as

$$f_2(z,t)=\frac{1}{\mu_2}\sum_{n=1}^{+\infty}a^{2n}B_n(t)z^{-n}+\frac{1}{\mu_2}\sum_{n=1}^{+\infty}[A_n(t)z^n-a^{2n}A_n(t)z^{-n}] -\frac{b_z}{2\pi}\ln\left(\frac{z-a^2/x_0}{z}\right)+\frac{b_z}{2\pi}\ln(z-x_0),\quad a<|z|<b \tag{10}$$

Next we address the outer viscous interface. It follows from Eq. (4*a*) for the continuity condition of traction across the outer viscous interface $|z|=b$ that

$$f_2(z,t)=\frac{\mu_3}{\mu_2}\bar{f}_3\left(\frac{b^2}{z},t\right)+\frac{1}{\mu_2}\sum_{n=1}^{+\infty}[C_n(t)z^n-b^{2n}C_n(t)z^{-n}] +\frac{b_z}{2\pi}\ln(z-x_0)-\frac{b_z}{2\pi}\ln(z-b^2/x_0)+\frac{b_z}{2\pi}\frac{\mu_3}{\mu_2}\ln z,\quad a<|z|<b$$

$$\bar{f}_2\left(\frac{b^2}{z},t\right)=\frac{\mu_3}{\mu_2}f_3(z,t)-\frac{1}{\mu_2}\sum_{n=1}^{+\infty}[C_n(t)z^n-b^{2n}C_n(t)z^{-n}] -\frac{b_z}{2\pi}\ln(z-x_0)+\frac{b_z}{2\pi}\ln(z-b^2/x_0)-\frac{b_z}{2\pi}\frac{\mu_3}{\mu_2}\ln z,\quad b<|z|<\frac{b^2}{a} \tag{11}$$

where $C_n(t)$ $(n=1,2,\ldots,+\infty)$ are real but time-dependent coefficients to be determined.

Substituting Eq. (11) into Eq. (4*b*), we obtain the following:

$$\frac{\mu_2+\mu_3}{\mu_2}\dot{\bar{f}}_3^{+}\left(\frac{b^2}{z},t\right)-\frac{\mu_3}{b\eta_b}\frac{b^2}{z}\bar{f}_3'^{+}\left(\frac{b^2}{z},t\right)+\frac{2}{\mu_2}\sum_{n=1}^{+\infty}\dot{C}_n(t)z^n =\frac{\mu_2+\mu_3}{\mu_2}\dot{f}_3^{-}(z,t)-\frac{\mu_3}{b\eta_b}zf_3'^{-}(z,t)+\frac{2}{\mu_2}\sum_{n=1}^{+\infty}b^{2n}\dot{C}_n(t)z^{-n},\quad |z|=b \tag{12}$$

Apparently the left-hand side of Eq. (12) is analytic and single valued within the circle $|z|=b$, while the right-hand side of Eq. (19) is analytic and single-valued outside the circle including the point at infinity. Again, by employing Liouville's theorem, the left- and right-hand sides should be identically zero. Consequently, we arrive at the following inhomogeneous first-order partial differential equation for $f_3(z,t)$:

$$zf_3'(z,t)-t_2\dot{f}_3(z,t)=\frac{2b\eta_b}{\mu_2\mu_3}\sum_{n=1}^{+\infty}b^{2n}\dot{C}_n(t)z^{-n},\quad |z|>b \tag{13}$$

where $t_2=b\eta_b(\mu_2+\mu_3)/\mu_2\mu_3>0$ is the characteristic time for the outer viscous interface $|z|=b$.

Equation (13) can also be solved by using power series expansion as

$$f_3(z,t)=\frac{b_z}{2\pi}\ln z+\frac{1}{\mu_3}\sum_{n=1}^{+\infty}D_n(t)z^{-n},\quad |z|>b \tag{14}$$

where $D_n(t)$ is related to $C_n(t)$ through

$$-nD_n(t)-t_2\dot{D}_n(t)=t_2\Gamma_2b^{2n}\dot{C}_n(t)\quad (n=1,2,\ldots,+\infty) \tag{15}$$

with $\Gamma_2=2\mu_3/(\mu_3+\mu_2)$ $(0\le\Gamma_2\le 2)$ being a measure of the relative stiffness of the matrix with respect to the interphase layer. It is of interest to observe from the above expression that as $t\to\infty$ $D_n(\infty)=0$. Consequently, $f_3(z,\infty)=(b_z/2\pi)\ln z$, which is the complex potential for a screw dislocation with Burgers vector b_z lodged within a circular hole of radius b.

Once we obtain $f_3(z,t)$, it is not difficult to arrive at another expression of $f_2(z,t)$ as

$$f_2(z,t)=\frac{1}{\mu_2}\sum_{n=1}^{+\infty}b^{-2n}D_n(t)z^n+\frac{1}{\mu_2}\sum_{n=1}^{+\infty}[C_n(t)z^n-b^{2n}C_n(t)z^{-n}] -\frac{b_z}{2\pi}\ln(z-b^2/x_0)+\frac{b_z}{2\pi}\ln(z-x_0),\quad a<|z|<b \tag{16}$$

Apparently the two expressions (10) and (16) for $f_2(z,t)$ should be exactly the same, from which we arrive at the following relations:

$$\sum_{n=1}^{+\infty}a^{2n}B_n(t)z^{-n}-\sum_{n=1}^{+\infty}a^{2n}A_n(t)z^{-n}+\sum_{n=1}^{+\infty}b^{2n}C_n(t)z^{-n} =\frac{\mu_2b_z}{2\pi}\ln\left(\frac{z-a^2/x_0}{z}\right)$$

$$\sum_{n=1}^{+\infty}b^{-2n}D_n(t)z^n-\sum_{n=1}^{+\infty}A_n(t)z^n+\sum_{n=1}^{+\infty}C_n(t)z^n =\frac{\mu_2b_z}{2\pi}\ln(z-b^2/x_0),\quad a<|z|<b \tag{17}$$

Therefore, from Eq. (17) the following set of algebraic equations for the unknowns can be obtained:

$$B_n(t)=A_n(t)-\left(\frac{b}{a}\right)^{2n}C_n(t)-\frac{\mu_2b_z}{2\pi}\frac{x_0^{-n}}{n}\quad (n=1,2,\ldots,+\infty)$$

$$D_n(t)=b^{2n}A_n(t)-b^{2n}C_n(t)-\frac{\mu_2b_z}{2\pi}\frac{x_0^{n}}{n}\quad (n=1,2,\ldots,+\infty) \tag{18}$$

Furthermore, using the relationships in Eq. (18), Eqs. (9) and (15) can be expressed, in terms of $A_n(t)$ and $C_n(t)$, into the following standard state-space equations:

$$\begin{bmatrix} t_1(\Gamma_1-1) & t_1\left(\frac{b}{a}\right)^{2n} \\ t_2 & t_2(\Gamma_2-1)\end{bmatrix}\begin{bmatrix}\dot{A}_n(t)\\ \dot{C}_n(t)\end{bmatrix}=n\begin{bmatrix}1 & -\left(\frac{b}{a}\right)^{2n}\\ -1 & 1\end{bmatrix}\begin{bmatrix}A_n(t)\\ C_n(t)\end{bmatrix} +\frac{\mu_2b_z}{2\pi}\begin{bmatrix}-x_0^{-n}\\ x_0^nb^{-2n}\end{bmatrix}\quad (n=1,2,\ldots,+\infty) \tag{19}$$

The general solutions to $A_n(t)$ and $C_n(t)$ can be obtained from the above equation as

$$A_n(t)=k_1^{(n)}\delta_{11}^{(n)}e^{-\lambda_1^{(n)}t}+k_2^{(n)}\delta_{12}^{(n)}e^{-\lambda_2^{(n)}t}+\rho_1^{(n)}$$

$$C_n(t)=k_1^{(n)}\delta_{21}^{(n)}e^{-\lambda_1^{(n)}t}+k_2^{(n)}\delta_{22}^{(n)}e^{-\lambda_2^{(n)}t}+\rho_2^{(n)}\quad (n=1,2,\ldots,+\infty) \tag{20}$$

where $\lambda_1^{(n)},\lambda_2^{(n)},\delta_{11}^{(n)},\delta_{12}^{(n)},\delta_{21}^{(n)},\delta_{22}^{(n)},\rho_1^{(n)},\rho_2^{(n)}$ are given by

$$\frac{\lambda_1^{(n)}}{n}=\frac{c_2^{(n)}+\sqrt{c_2^{(n)2}-4c_1^{(n)}c_3^{(n)}}}{2c_1^{(n)}}>0,$$

$$\frac{\lambda_2^{(n)}}{n}=\frac{c_2^{(n)}-\sqrt{c_2^{(n)2}-4c_1^{(n)}c_3^{(n)}}}{2c_1^{(n)}}>0 \tag{21a}$$

$$\delta_{11}^{(n)} = \lambda_1^{(n)} t_2(\Gamma_2 - 1) + n, \quad \delta_{21}^{(n)} = n - \lambda_1^{(n)} t_2$$

$$\delta_{12}^{(n)} = \lambda_2^{(n)} t_2(\Gamma_2 - 1) + n, \quad \delta_{22}^{(n)} = n - \lambda_2^{(n)} t_2 \tag{21b}$$

$$\rho_1^{(n)} = \frac{\mu_2 b_z (x_0^n a^{-2n} - x_0^{-n})}{2\pi n c_3^{(n)}}, \quad \rho_2^{(n)} = \frac{\mu_2 b_z (x_0^n b^{-2n} - x_0^{-n})}{2\pi n c_3^{(n)}} \tag{21c}$$

with

$$c_1^{(n)} = t_1 t_2 (c_3^{(n)} - \Gamma_1\Gamma_2 + \Gamma_1 + \Gamma_2),$$

$$c_2^{(n)} = t_1\Gamma_1 + t_2\Gamma_2 + c_3^{(n)}(t_1 + t_2),$$

$$c_3^{(n)} = \left(\frac{b}{a}\right)^{2n} - 1 \tag{22}$$

and $k_1^{(n)}$ and $k_2^{(n)}$ are related to the initial conditions of $A_n(t)$ and $C_n(t)$ through the following:

$$k_1^{(n)} = \frac{\delta_{22}^{(n)} A_n(0) - \delta_{12}^{(n)} C_n(0) + \delta_{12}^{(n)} \rho_2^{(n)} - \delta_{22}^{(n)} \rho_1^{(n)}}{\delta_{11}^{(n)} \delta_{22}^{(n)} - \delta_{12}^{(n)} \delta_{21}^{(n)}} \quad (n = 1,2, \ldots, +\infty)$$

$$k_2^{(n)} = \frac{\delta_{11}^{(n)} C_n(0) - \delta_{21}^{(n)} A_n(0) + \delta_{21}^{(n)} \rho_1^{(n)} - \delta_{11}^{(n)} \rho_2^{(n)}}{\delta_{11}^{(n)} \delta_{22}^{(n)} - \delta_{12}^{(n)} \delta_{21}^{(n)}} \quad (n = 1,2, \ldots, +\infty) \tag{23}$$

At the initial moment $t=0$ when the screw dislocation is just introduced into the interphase layer, the displacement across the viscous interface has no time to experience any jump [15]. Consequently, both the inner interface $r=a$ and the outer interface $r=b$ are perfect at $t=0$, i.e., the traction and displacement are both continuous across the two interfaces at the initial moment $t=0$. Then we can easily obtain the initial values of $A_n(t)$ and $C_n(t)$ as

$$A_n(0) = \frac{\mu_2 b_z (1 - \Gamma_2)[x_0^n a^{-2n} - (1 - \Gamma_1) x_0^{-n}]}{2\pi n (c_3^{(n)} + \Gamma_1 + \Gamma_2 - \Gamma_1\Gamma_2)},$$

$$C_n(0) = \frac{\mu_2 b_z (1 - \Gamma_1)[(1 - \Gamma_2) x_0^n b^{-2n} - x_0^{-n}]}{2\pi n (c_3^{(n)} + \Gamma_1 + \Gamma_2 - \Gamma_1\Gamma_2)} \quad (n = 1,2, \ldots, +\infty) \tag{24}$$

It is observed that, when $\Gamma_1=\Gamma_2=0$, we have $\rho_1^{(n)}=A_n(0)$ and $\rho_2^{(n)}=C_n(0)$. This fact is easy to understand. It follows from Eq. (20) that $A_n(\infty)=\rho_1^{(n)}$ and $C_n(\infty)=\rho_2^{(n)}$. When $t\to\infty$ the two viscous interfaces become traction-free surfaces, while traction-free surfaces can also be obtained by assuming the shear moduli of the inhomogeneity and the matrix to be zero ($\Gamma_1=\Gamma_2=0$). Now the unknowns $A_n(t)$ and $C_n(t)$ have been uniquely determined. The other unknowns $B_n(t)$ and $D_n(t)$ can then be uniquely obtained from Eq. (18).

The time-dependent stresses in the composite induced by the screw dislocation can then be given by

$$\sigma_{zy}^{(1)} + i\sigma_{zx}^{(1)} = \sum_{n=1}^{+\infty} n B_n(t) z^{n-1}, \quad |z| < a \tag{25}$$

$$\sigma_{zy}^{(2)} + i\sigma_{zx}^{(2)} = \sum_{n=1}^{+\infty} n[A_n(t)(z^{n-1} + a^{2n} z^{-n-1}) - a^{2n} B_n(t) z^{-n-1}] - \frac{\mu_2 b_z}{2\pi} \frac{a^2}{z(x_0 z - a^2)} + \frac{\mu_2 b_z}{2\pi} \frac{1}{z - x_0}, \quad a < |z| < b \tag{26}$$

$$\sigma_{zy}^{(3)} + i\sigma_{zx}^{(3)} = -\sum_{n=1}^{+\infty} n D_n(t) z^{-n-1} + \frac{\mu_3 b_z}{2\pi z}, \quad |z| > b \tag{27}$$

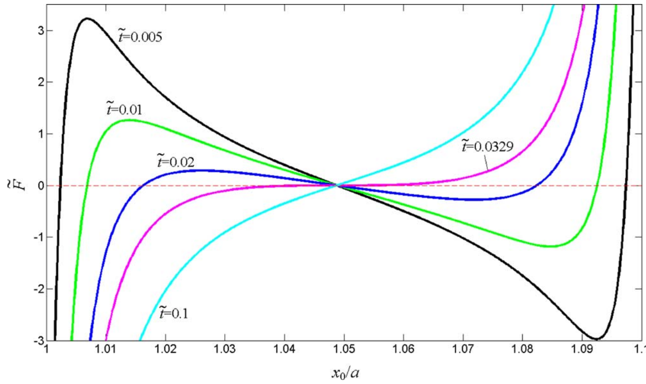

Fig. 2 The normalized time-dependent image force $\tilde{F}=aF_x/\mu_2 b_z^2$ on the screw dislocation at five different times $\tilde{t}=t/t_0=0.005$, 0.01, 0.02, 0.0329, 0.1 with $t_1=t_2=t_0$, $\Gamma_1=\Gamma_2=\Gamma=1.8$, and $b=1.1a$

It is obvious that the stresses are singular at the location of the screw dislocation $z=x_0$.

3 Time-Dependent Image Force on the Screw Dislocation

By employing the Peach–Koehler formula (see, for example, Refs. [16,17]), the time-dependent image force on the screw dislocation due to its interaction with the two viscous interfaces can be finally obtained as

$$F_x(t) = b_z \sum_{n=1}^{+\infty} n[k_1^{(n)}(\delta_{11}^{(n)} x_0^{n-1} + \delta_{21}^{(n)} b^{2n} x_0^{-n-1})\exp(-\lambda_1^{(n)} t) + k_2^{(n)} \times(\delta_{12}^{(n)} x_0^{n-1} + \delta_{22}^{(n)} b^{2n} x_0^{-n-1})\exp(-\lambda_2^{(n)} t) + x_0^{n-1}\rho_1^{(n)} + b^{2n} x_0^{-n-1} \rho_2^{(n)}] \quad (a < x_0 < b) \tag{28}$$

where F_x is the x component of the image force while $F_y=0$. During calculation the infinite series in Eq. (28) is truncated at a large integer $n=N$ to get sufficiently accurate result.

Apparently it follows from Eq. (28) that

$$F_x(0) = b_z \sum_{n=1}^{+\infty} n[x_0^{n-1} A_n(0) + b^{2n} x_0^{-n-1} C_n(0)] \tag{29}$$

is the image force on the screw dislocation interacting with two perfect interfaces, while

$$F_x(\infty) = b_z \sum_{n=1}^{+\infty} n[x_0^{n-1}\rho_1^{(n)} + b^{2n} x_0^{-n-1}\rho_2^{(n)}] = b_z \sum_{n=1}^{+\infty} n[x_0^{n-1} A_n(\infty) + b^{2n} x_0^{-n-1} C_n(\infty)] \tag{30}$$

is the image force on the screw dislocation interacting with two traction-free surfaces. In addition, it can be strictly proved from Eq. (28) that when the inhomogeneity and the matrix possess the same shear modulus, i.e., $\Gamma_1=\Gamma_2=\Gamma$, and the characteristic times for the two viscous interfaces are exactly the same, i.e., $t_1=t_2=t_0$, then the fixed location $x_0=\sqrt{ab}$ is always an equilibrium position for the dislocation at any time, i.e., $F_x(t)\equiv 0$ when $x_0=\sqrt{ab}$. Apparently when the interphase layer is stiffer than both the inhomogeneity and the matrix, i.e., $\Gamma\le 1$, the fixed equilibrium position is always an unstable one. On the other hand, when the interphase layer is more compliant than both the inhomogeneity and the matrix, i.e., $\Gamma>1$, the nature of the fixed equilibrium position is dependent on time. In the following calculations, we truncate the series in Eq. (28) at $n=360$ to obtain a result with a relative truncation error less than 0.01%. We illustrate in Fig. 2 the

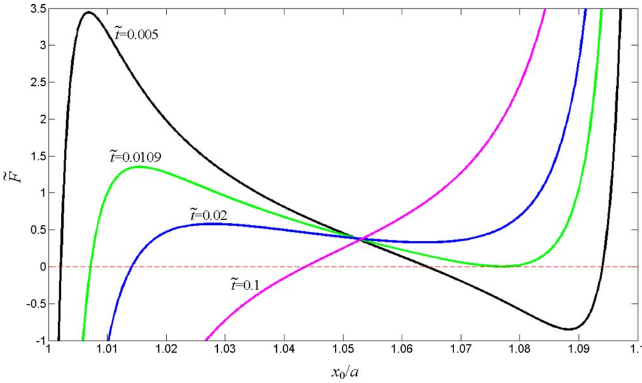

Fig. 3 The normalized time-dependent image force $\tilde{F} = aF_x/\mu_2 b_z^2$ on the screw dislocation at four different times $\tilde{t} = t/t_0 = 0.005$, 0.0109, 0.02, 0.1 with $t_1 = t_2 = t_0$, $\Gamma_1 = 1.8$, $\Gamma_2 = 1.5$, and $b = 1.1a$

normalized image force $\tilde{F} = aF_x/\mu_2 b_z^2$ at five different times $\tilde{t} = t/t_0 = 0.005$, 0.01, 0.02, 0.0329, 0.1 with $\Gamma = 1.8 > 1$ and $b = 1.1a$. It is clearly observed from Fig. 2 that (i) $x_0 = \sqrt{ab} = 1.0488a$ is always an equilibrium position, and this fixed equilibrium position is a stable one when $\tilde{t} < 0.0329$ and it is an unstable one when $\tilde{t} > 0.0329$; (ii) two unstable and one stable transient equilibrium positions for the dislocation coexist when $\tilde{t} < 0.0329$, while only one fixed equilibrium position exists when $\tilde{t} > 0.0329$. Next we consider the more general case in which $\Gamma_1 \neq \Gamma_2$ (for simplification we still assume that $t_1 = t_2 = t_0$). Figure 3 demonstrates the normalized image force $\tilde{F} = aF_x/\mu_2 b_z^2$ at four different times $\tilde{t} = t/t_0 = 0.005$, 0.0109, 0.02, 0.1 with $\Gamma_1 = 1.8$, $\Gamma_2 = 1.5$, and $b = 1.1a$. It is observed from Fig. 3 that (i) two unstable and one stable transient equilibrium positions for the dislocation coexist when $\tilde{t} < 0.0109$, (ii) a saddle point (neither stable nor unstable) transient equilibrium position at $x_0 \approx 1.078a$ and another unstable transient equilibrium position coexist when $\tilde{t} = 0.0109$, and (iii) only one single unstable transient equilibrium position exists when $\tilde{t} > 0.0109$ and the single unstable transient equilibrium position moves toward $x_0 = \sqrt{ab} = 1.0488a$ as the time evolves. As a comparison to Fig. 3, Fig. 4 demonstrates the normalized image force $\tilde{F} = aF_x/\mu_2 b_z^2$ at four different times $\tilde{t} = t/t_0 = 0.005$, 0.0109, 0.02, 0.1 with $\Gamma_1 = 1.5$, $\Gamma_2 = 1.8$, and $b = 1.1a$. It is observed that Fig. 4 has very similar features as Fig. 3. For instance, when $\tilde{t} = 0.0109$ we also observe from Fig. 4 a saddle point transient equilibrium position at $x_0 \approx 1.021a$. The above results indicate that the situations for the transient equilibrium positions are rather complex and are dependent on Γ_1 and Γ_2 and the chosen time. We show in Fig. 5 the different situations for the transient equilibrium positions of the dislocation at a certain fixed normalized time $\tilde{t} = t/t_0$ with the assumption that $t_1 = t_2 = t_0$ and $b = 1.1a$. It is observed from Fig. 5 that (i) when $[\Gamma_1, \Gamma_2]$ is just located on the curve for a certain normalized time $\tilde{t}$, a saddle point and another unstable transient equilibrium positions coexist at this normalized time; (ii) when $[\Gamma_1, \Gamma_2]$ is located within the region formed by the curve for a certain fixed normalized time $\tilde{t}$ and the two straight lines $\Gamma_1 = 2$ and $\Gamma_2 = 2$, two unstable and one stable transient equilibrium positions for the dislocation coexist at this normalized time; (iii) otherwise, for other combinations of $[\Gamma_1, \Gamma_2]$ only one unstable transient equilibrium position exists at this normalized time; (iv) if $[\Gamma_1, \Gamma_2]$ is on the curve for a certain normalized time $\tilde{t}$, then $[\Gamma_2, \Gamma_1]$ is also on this curve; and (v) it is only possible to find a single unstable transient equilibrium position if $\tilde{t} > \tilde{t}_c = 0.03983$. The results in Fig. 5 imply that there exist simultaneously three transient equilibrium positions if the interphase layer is more compliant than both the inhomogeneity and the matrix and the time chosen is fast enough. Figure 5 also indicates that there exists only one unstable transient equilibrium position if the time chosen is above a critical value no matter how stiff the inhomogeneity and the matrix are. Here it is of interest to look into the dependence of $\tilde{t}_c$ on the thickness of the interphase layer in more detail with the assumption that $t_1 = t_2 = t_0$. We present in Fig. 6 the variation in $\tilde{t}_c$ as a function of the relative thickness $(b-a)/a$ of the interphase layer. It is observed from Fig. 6 that (i) $\tilde{t}_c$ is an increasing function of $(b-a)/a$ and (ii) $\tilde{t}_c$ approaches zero as the interphase layer is infinitely thin (i.e., $b \to a$), and it approaches $\ln 2 = 0.6931$ as the interphase layer is infinitely thick (i.e., $(b-a)/a \to \infty$). It is of interest to notice that the asymptotic behavior of $\tilde{t}_c \to \ln 2$ as $(b-a)/a \to \infty$ is in agreement with our previous exact result for a single viscous interface [11]. The results in Fig. 6 imply that it is only possible to find a single unstable transient equilibrium position if $\tilde{t} > \ln 2$ no matter how thick the interphase layer is.

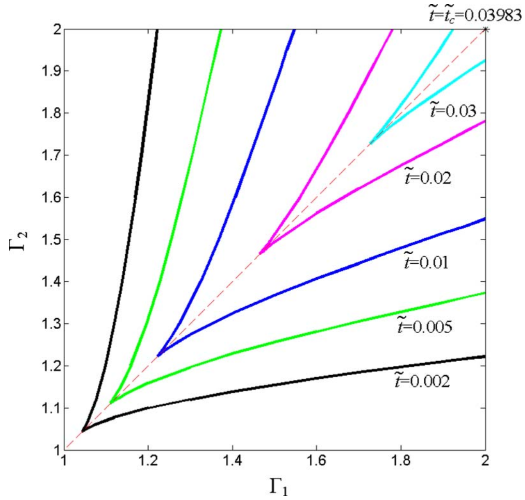

Fig. 5 The different situations for the transient equilibrium positions of the dislocation at a certain fixed normalized time $\tilde{t} = t/t_0$ with $t_1 = t_2 = t_0$ and $b = 1.1a$

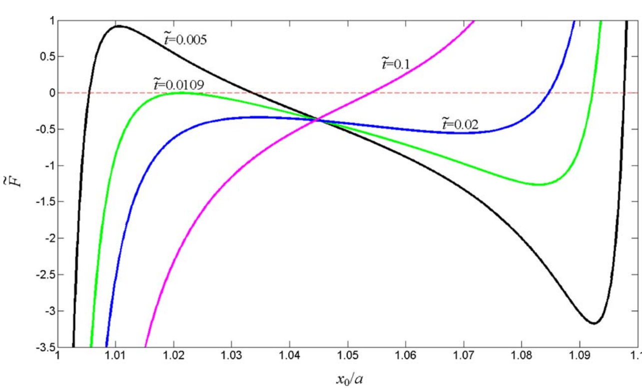

Fig. 4 The normalized time-dependent image force $\tilde{F} = aF_x/\mu_2 b_z^2$ on the screw dislocation at four different times $\tilde{t} = t/t_0 = 0.005$, 0.0109, 0.02, 0.1 with $t_1 = t_2 = t_0$, $\Gamma_1 = 1.5$, $\Gamma_2 = 1.8$, and $b = 1.1a$

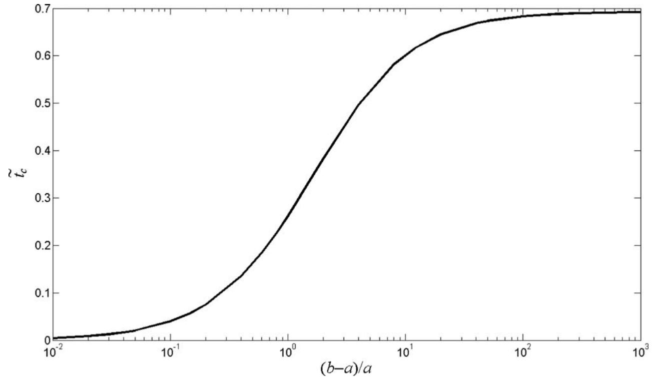

Fig. 6 The variation in $\tilde{t}_c$ as a function of the relative thickness $(b-a)/a$ of the interphase layer with the assumption that $t_1=t_2=t_0$

4 Conclusions

We investigated the problem associated with a screw dislocation interacting with two concentric linear viscous interfaces by means of the complex variable method. The time-dependent stress field and image force acting on the dislocation due to its interaction with the two viscous interfaces were derived. Our results demonstrated that three situations are possible for the transient equilibrium positions depending on the relative stiffness among the three material phases and the time chosen: (i) two unstable and one stable transient equilibrium positions coexist, (ii) a saddle point and an unstable transient equilibrium positions coexist, and (iii) only one single unstable transient equilibrium position exists. The image force as a function of these parameters was presented numerically to illustrate these features, along with the criterion diagrams for determining the specific situation for the transient equilibrium positions.

Acknowledgment

This work was partially supported by AFRL and ARL grants. The authors would like to thank the reviewers for their constructive comments.

References

[1] Ru, C. Q., 1999, "Three-Phase Elliptical Inclusions With Internal Uniform Hydrostatic Stresses," J. Mech. Phys. Solids, **47**, pp. 259–273.

[2] Liu, Y. J., Xu, N., and Luo, J. F., 2000, "Modeling of Interphases in Fiber-Reinforced Composites Under Transverse Loading Using the Boundary Element Method," ASME J. Appl. Mech., **67**, pp. 41–49.

[3] Xiao, Z. M., and Chen, B. J., 2000, "A Screw Dislocation Interacting With a Coated Fiber," Mech. Mater., **32**, pp. 485–494.

[4] Raj, R., and Ashby, M. F., 1971, "On Grain Boundary Sliding and Diffusional Creep," Metall. Trans., **2**, pp. 1113–1127.

[5] Ke, T. S., 1999, "Fifty-Year Study of Grain-Boundary Relaxation," Metall. Mater. Trans. A, **30**, pp. 2267–2295.

[6] Ashby, M. F., 1972, "Boundary Defects and Atomistic Aspects of Boundary Sliding and Diffusional Creep," Surf. Sci., **31**, pp. 498–542.

[7] Suo, Z., 1997, "Motion of Microscopic Surface in Materials," Adv. Appl. Mech., **33**, pp. 193–294.

[8] Nagarajan, R., Dutta, I., Funn, J. V., and Esmele, M., 1999, "Role of Interfacial Sliding on the Longitudinal Creep Response of Continuous Fiber Reinforced Metal-Matrix Composite," Mater. Sci. Eng., A, **259**, pp. 237–252.

[9] He, L. H., and Lim, C. W., 2001, "Time-Dependent Interfacial Sliding in Fiber Composites Under Longitudinal Shear," Compos. Sci. Technol., **61**, pp. 579–584.

[10] He, L. H., and Lim, C. W., 2003, "Electromechanical Responses of Piezoelectric Fiber Composites With Sliding Interface Under Anti-Plane Deformations," Composites, Part B, **34**, pp. 373–381.

[11] Wang, X., Pan, E., and Roy, A. K., 2008, "Interaction Between a Screw Dislocation and a Piezoelectric Circular Inclusion With Viscous Interface," J. Mech. Mater. Struct., **3**(4), pp. 761–773.

[12] Wang, X., Pan, E., and Albrecht, J. D., 2008, "Two-Dimensional Green's Functions in Anisotropic Multiferroic Bimaterials With Viscous Interface," J. Mech. Phys. Solids, **56**, pp. 2863–2875.

[13] Lauhon, L. J., Gudiksen, M. S., Wang, D. L., and Lieber, C. M., 2002, "Epitaxial Core-Shell and Core Multishell Nanowire Heterostructures," Nature (London), **420**, pp. 57–61.

[14] Muskhelishvili, N. I., 1953, *Some Basic Problems of the Mathematical Theory of Elasticity*, Noordhoff, Groningen.

[15] Fan, H., and Wang, G. F., 2003, "Interaction Between a Screw Dislocation and Viscoelastic Interfaces," Int. J. Solids Struct., **40**, pp. 763–776.

[16] Ohr, S. M., Chang, S. J., and Thomson, R., 1985, "Elastic Interaction of a Wedge Crack With a Screw Dislocation," J. Appl. Phys., **57**, pp. 1839–1843.

[17] Lee, K. Y., Lee, W. G., and Pak, Y. E., 2000, "Interaction Between a Semi-Infinite Crack and a Screw Dislocation in a Piezoelectric Material," ASME J. Appl. Mech., **67**, pp. 165–170.